

SIMULATION STUDIES OF THE DIELECTRIC GRATING AS AN ACCELERATING AND FOCUSING STRUCTURE*

K. Soong[†], E. A. Peralta[‡], R. L. Byer, Stanford University, Stanford, CA 94305, USA
E. Colby, SLAC National Accelerator Laboratory, Menlo Park, CA 94025, USA

Abstract

A grating-based design is a promising candidate for a laser-driven dielectric accelerator. Through simulations, we show the merits of a readily fabricated grating structure as an accelerating component. Additionally, we show that with a small design perturbation, the accelerating component can be converted into a focusing structure. The understanding of these two components is critical in the successful development of any complete accelerator.

INTRODUCTION

The concept of accelerating electrons with the tremendous electric fields found in lasers has been proposed for decades. However, until recently the realization of such an accelerator was not technologically feasible. Recent advances in the semiconductor industry, as well as advances in laser technology, have now made laser-driven dielectric accelerators imminent. The grating-based accelerator is one proposed design for a dielectric laser-driven accelerator. This design, which was introduced by Plettner [1], consists of a pair of opposing transparent binary gratings, illustrated in Fig. 1. The teeth of the gratings serve as a phase mask, ensuring a phase synchronicity between the electromagnetic field and the moving particles.

The current grating accelerator design has the drive laser incident perpendicular to the substrate, which poses a laser-structure alignment complication [2]. The next iteration of grating structure fabrication seeks to monolithically create an array of grating structures by etching the grating's vacuum channel into a fused silica wafer. With this method it is possible to have the drive laser confined to the plane of the wafer, thus ensuring alignment of the laser-and-structure, the two grating halves, and subsequent accelerator components.

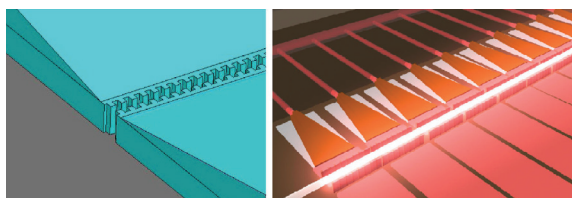


Figure 1: An illustration of a single grating structure (left) as well as a staged array of grating structures (right). Illustration courtesy of Di Xu of SLAC.

* Work supported by DOE contract DE-AC02-76SF00515 (SLAC)

[†] kensoong@stanford.edu

[‡] eperalta@stanford.edu

There has been previous work using 2-dimensional finite difference time domain (2D-FDTD) calculations to evaluate the performance of the grating accelerator structure [1]. However, this work approximates the grating as an infinite structure and does not accurately model a realizable structure. In this paper, we will present a 3-dimensional frequency-domain simulation of both the infinite and the finite grating accelerator structure. Additionally, we will present a new scheme for a focusing structure based on a perturbation of the accelerating structure. We will present simulations of this proposed focusing structure and quantify the quality of the focusing fields.

ACCELERATION STRUCTURE

The original design of the grating accelerator structure optimized the grating geometry to maximize the resulting acceleration gradient. For a fused silica accelerating structure driven at 800nm (λ); a pillar depth of $.9 \lambda$ and a grating separation of $.25 \lambda$ was found to give a maximum unloaded gradient of $G_{0,max} \sim .24|E_{max}|$ [1]. The prior mentioned 2D-FDTD code has been recently used to calculate the effect of fabrication-induced deviations from design. For example, the current fabricated gratings have rounded edges and the stacked structure may be prone to longitudinal misalignment [2]. The expected gradient from such a structure was calculated to be $G_0 \sim .138|E_{max}|$ (58% of ideal maximum value) with our 2D-FDTD code using a grating profile extracted from SEM images, as shown in Figure 2.

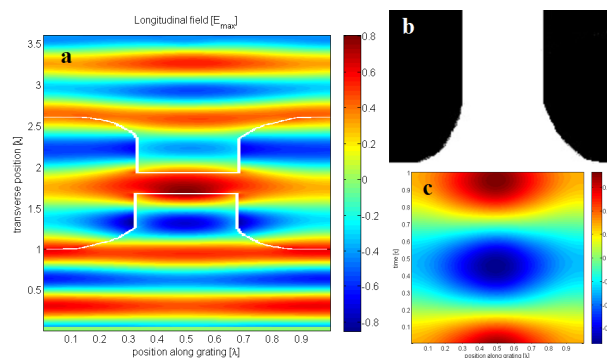


Figure 2: a. 2D-FDTD calculated longitudinal field in our current structures. b. Extracted SEM cross-section used in the model. c. Longitudinal fields in the channel center.

Further simulations with the rounded-edge geometry show that the resulting acceleration gradient can be increased to 73% of $G_{0,max}$ by etching the gratings to their optimal depth of 720nm. The effect of longitudinal mis-

alignment was also studied with FDTD simulations by varying the position of the top grating as illustrated on the left part of Figure 3. It is clear from this calculation that two gratings need not be exactly aligned longitudinally to achieve a significant gradient; even at its worst longitudinal alignment (with the gratings off by $\lambda/4$), the resulting accelerating gradient is still 75 % of $G_{0,max}$. However, such a misalignment may produce significant beam-degrading effects which we'll investigate in the near future.

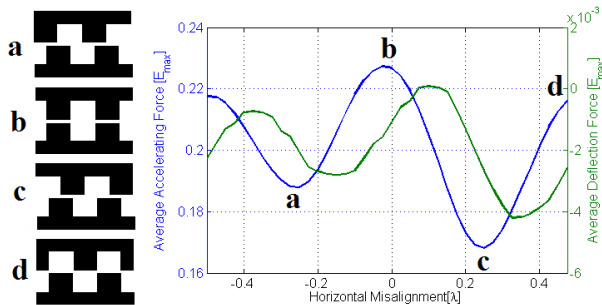


Figure 3: Effect of grating misalignment of the resulting acceleration gradient and deflection force

To ensure that our 3D, frequency-domain, finite element simulations using the code HFSS produce accurate results, we simulate the exact structure from the original design in Ref. [1]. The results are juxtaposed in Figure 4 where we can see that the resulting fields are both qualitatively and quantitatively similar. The computed gradient for the HFSS simulations is $G_0 \sim .21|E_{max}|$, compared to $G_0 \sim .24|E_{max}|$ from FDTD.

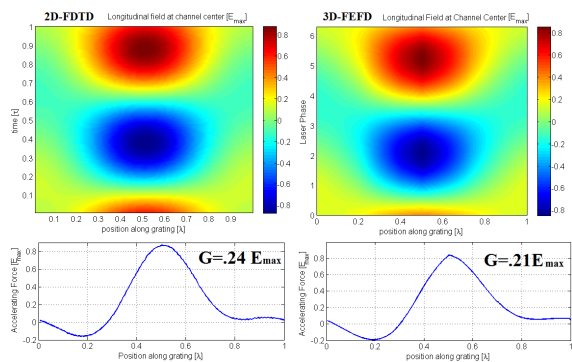


Figure 4: Comparison of 2D-FDTD (left) and 3D-FEFD (right) simulation of the original structure from Ref. [1].

Having benchmarked the computation software, we computed the fields in a finite grating structure, something impossible to do with the 2D-FDTD code. The grating geometry was identical to Ref. [1] with the exception of a finite grating of width $1 \mu\text{m}$ in a fused silica substrate. A single period structure is modeled with periodic boundary conditions and perfectly matched layers enclosing the computation region. The resulting fields in the vacuum channel are integrated along the longitudinal direction and shown in Figure 5.

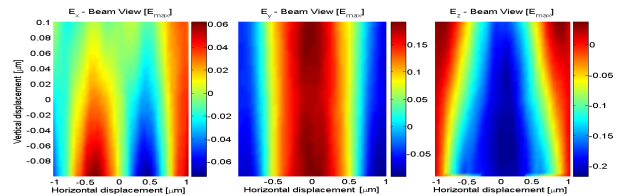


Figure 5: Longitudinally-integrated fields in the vacuum channel of a $1 \mu\text{m}$ wide grating structure like that of [1].

It is evident from the plot of E_y in Figure 5 (center) that an accelerating field is present in the center of the vacuum channel. This field has a peak value of $\sim .175|E_{max}|$ (83% of $G_{0,max}$) but decreases away from the center to a value of $\sim .069|E_{max}|$ at the edge of the grating.

FOCUSING STRUCTURE

A complete dielectric accelerator design will require focusing structures, in order to confine the accelerated particle beam. Magneto-static focusing structures are bulky and difficult to implement in conjunction with the dielectric accelerating structures and are therefore neglected in favor of an all-dielectric electromagnetic focusing structure. In addition to possessing two-to-three orders of magnitude greater focusing gradients, dielectric quadrupoles can be lithographically develop along-side the accelerating structures to achieve nanometer-class alignment accuracy.

A dielectric focusing structure based on a variant of the grating accelerator has previously been proposed [3], but this structure design is incompatible with our proposed accelerator fabrication procedure. In light of this, we propose a new design for a grating-based focusing structure that is geometrically identical to the accelerating structure, with the exception of the relative lengths of its features. As a result of the high level of similarity, it will be possible to fabricate both structures monolithically and with the same process flow.

The geometry of the focusing structure is illustrated in Fig. 6, with the Y-axis serving as the direction of acceleration. A focusing field is achieved by adjusting the height of the grating teeth, the gap between gratings, and the width of the input coupler. The profile of this focusing field can be tailored to the beam profile with proper adjustments of these three parameters. In this paper, we present a design specifically for the case of a round beam.

We simulated the focusing structure design using the frequency domain solver HFSS. For this particular design, we set the period of the structure to 800nm, the height of the grating teeth to 300nm, the gap between gratings to 200nm, and the width of the input coupler to 1000nm. Planewaves with electric fields along the Y-axis were incident symmetrically from the top and the bottom of the grating structure, shown as the red region in Fig. 6. This can be achieved in practice by attaching a tapered waveguide to the grating structure at the location of the incident planewave, similar

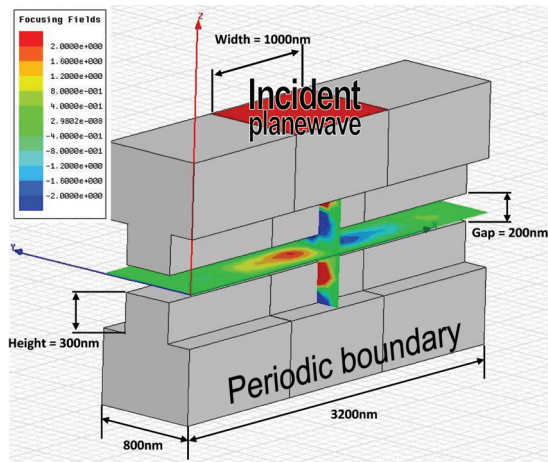


Figure 6: An illustration of the geometry of the focusing structure with the Y-axis serving as the direction of beam propagation.

to the design of Fig. 1.

The integrated radial focusing force for a phase-synchronous particle is shown in Fig. 7. More specifically, Fig. 7 is a map of the integral, $\int_0^{\lambda_g} (F \cdot \hat{r}) dy$, where F is the electro-magnetic force, \hat{r} is the unit radial vector, and λ_g is the grating period.

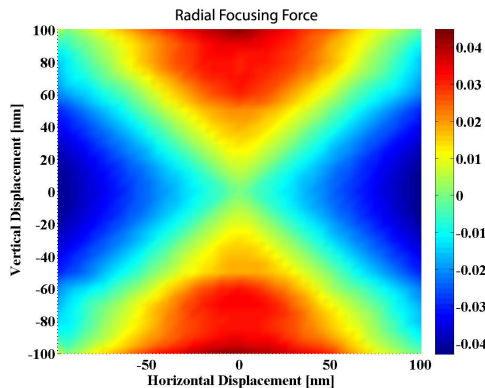


Figure 7: A map of the radial focusing force experienced by a phase synchronous particle.

It is evident from the field map that a quadrupole-like focusing field exists. To quantify the quality of the quadrupole focusing field, we examined the multipole content of the radial fields. We performed a Fourier transform on the radial fields along a fixed radius and extrapolated the relative strength of each multipole. The relative strength of the first seven multipoles at a radius of 100nm is shown in Fig. 8. Through this analysis, we found the quadrupole component to be dominate by two-orders of magnitude. We obtained similar results when examining the multipole content at other radii.

From experimental damage threshold measurements of a prototype silica accelerator [4] in conjunction with HFSS simulations, we calculate that a single period of this focus-

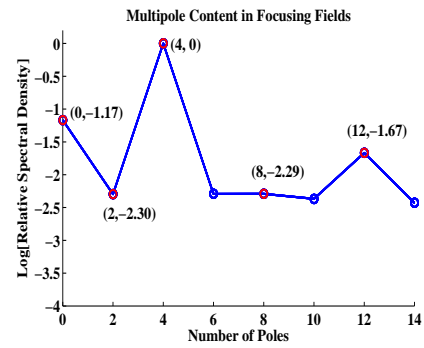


Figure 8: Multipole content of the focusing field, as determined by a Fourier transform of the radial fields along a fixed radius, $r=100\text{nm}$.

ing structure can sustain a radial field gradient in excess of 0.4 MT/m.

CONCLUSION

In this paper we have examined the performance of a grating-based dielectric accelerator. We found that a finite grating structure performs quantitatively similar to the infinite grating approximation. Additionally, we have shown that fabrication imperfections in the grating structure does not severely inhibit the performance of the structure as an accelerator. Based on experimental measurements, we calculate a sustainable accelerating gradient in excess of 600MV/m. Additionally, we have presented a new concept for a focusing structure, that shares many of the same geometric features as the grating accelerator. We have shown that this focusing structure is capable of generating a quadrupole focusing field with little higher-order multipole contamination. Based on experimental measurements, we calculate a radial focusing gradient in excess of 0.4MT/m. Future simulation work will involve 3D simulations of the geometrically-imperfect fabricated grating structure. Additionally, future work will seek to improve the aperture and gradient of the focusing structure, as well as design a focusing structure for sheet beams. The ultimate goal of this project will be to simulate a multi-stage accelerator, including accelerating and focusing structures, as well as, waveguides, couplers, and various other accelerator components.

REFERENCES

- [1] T. Plettner et al., Phys. Rev. STAB 9 (2006) 111301.
- [2] E. A. Peralta et al., "Fabrication and Measurement of Silica Grating Accelerator Structures," PAC, MOP096 (2011).
- [3] T. Plettner et al., Phys. Rev. STAB 12 (2009) 101302.
- [4] K. Soong, et al., "Experimental Determination of Damage Threshold Characteristics of IR Compatible Optical Materials," PAC 11, MOP095 (2011).